Journal of Solid State Chemistry **155,** 238–242 (2000)
doi:10.1006/jssc.2000.8947, available online at http://www.idealibrary.com on IDEAL®

Hybrid Open Frameworks. Hydrothermal Synthesis, Structure Determinations, and Magnetic Behavior of $(V^{IV}O)_2(H_2O)\{O_3P–(CH_2)_3–PO_3\}\cdot 2H_2O$: A New Vanado-alkyldiphosphonate Closely Related to $VO(HPO_4)\cdot 0.5H_2O$

D. Riou,*,[1] C. Serre,* J. Provost†, and G. Ferey*

*Institut Lavoisier UMR CNRS 8637, Université de Versailles-St Quentin, 45 Avenue des Etats-Unis, 78035 Versailles Cedex, France; and †Laboratoire CRISMAT-ISMRa UMR 6508, 6 Boulevard Maréchal Juin, 14050 Caen Cedex, France

DEDICATED TO PROFESSOR J. M. HONIG

$(V^{IV}O)_2(H_2O)\{O_3P–(CH_2)_3–PO_3\}\cdot 2H_2O$ was hydrothermally synthesized from a mixture of $VOSO_4\cdot 5H_2O : H_2PO_3–(CH_2)_3–PO_3H_2 : H_2O$ in a molar ratio 1 : 0.5 : 250 and heated for 72 hours to 170°C. Its structure was determined from powder X-ray diffraction data. It crystallizes in the orthorhombic space group *Immm* (No. 71) with $a = 16.8210(5)$ Å, $b = 9.3790(3)$ Å, $c = 7.4568(2)$ Å, $V = 1176.4(1)$ Å^3, $Z = 4$. The pillared framework is built up from inorganic layers covalently linked via P–C–C–C–P bonds. The inorganic layers are similar to those encountered in a $VO(HPO_4)\cdot 0.5H_2O$ bidimensional compound described previously. The dimers of face-shared $VO_5(H_2O)$ octahedra are linked by PO_3C phosphonate groups instead of $PO_3(OH)$ groups in the vanadyl hydrogenphosphate. The terminal hydroxyl groups in the latter are substituted by the carbons of the organic chains which link two layers, giving the three-dimensional character of the structure. The magnetic behaviors of the two compounds are compared. © 2000 Academic Press

Key Words: **Hydrothermal synthesis; phosphonate compounds; magnetic properties.**

INTRODUCTION

For 10 years, many papers have addressed the hydrothermal synthesis of organically templated metallophosphates with open frameworks (1). However, only a few of these compounds are really microporous, the removal of the template often leading to the collapse of the structure. The hybrid route, known for some years (2–8), was an attempt to suppress this drawback. It involves replacing phosphate groups by functionalized alkyl chains, the grafting functions (phosphonates, carboxylates, sulfonates, or a mixture of them) playing the same chelating role as PO_4^{3-}. This method also has the advantage of playing on the length of the alkyl chains to modulate the dimensions of the cavity which is rendered hydrophobic to some extent. When the metallic cation is vanadium, only a few hybrid compounds are known up to now. The main results were obtained by the groups of Zubieta, Jacobson, and ours. The two former groups have described some layered compounds formed from monophosphonic precursors (9–15) whereas three-dimensional frameworks are obtained solely with diphosphonic acids (16). Vanadium is often in the tetra- or pentavalent oxidation state but some vanado(III)-diphosphonates have been prepared at higher temperatures ($250 \le T \le 300$°C) (17) or in the presence of a reducing agent such as an amine which here does not act as a template (18). Our contribution addresses the hydrothermal synthesis and the structure determination of new vanadoalkyldiphosphonate compounds labeled MIL-2 (19) and MIL-10 (20) when the alkyl chain possesses one carbon atom, MIL-3 (19) and MIL-5 (21) for two carbons, and MIL-7 LT and HT (22) with the propylenediphosphonic precursor.

This paper describes the synthesis and structure of a new pillared compound build up by stacking inorganic slabs closely related to those encountered in $VO(HPO_4)\cdot 0.5H_2O$ (23) and linked by the propyl chains. The magnetic behavior of $(V^{IV}O)_2(H_2O)\{O_3P–(CH_2)_3–PO_3\}\cdot 2H_2O$ is discussed.

EXPERIMENTAL

Hydrothermal Synthesis and Chemical Analysis

The title compound was hydrothermally synthesized from a mixture of 0.2812 g of $VOSO_4\cdot 5H_2O$ (Prolabo), 0.1056 g of $H_2O_3P–(CH_2)_3–PO_3H_2$ (Alfa), and 5 ml of deionized water (molar ratio 1 : 0.5 : 250). The mixture was sealed in a Parr Teflon-lined steel autoclave for 2 days at 170°C and then slowly cooled (3 days) to room temperature. The resultant product (yield ≈ 75% relative to vanadium) appears as a light blue powder which can be separated from

[1]To whom correspondence should be addressed.

0022-4596/00 $35.00

the liquid by filtration and then washed with water. The pH remained equal to 1 throughout the synthesis.

The density of the powder was measured with a Micromeritics multipycnometer operating under He flow. Complementary thermogravimetric analyses were performed under O_2 atmosphere with a TA Instruments TGA 2050 apparatus (heating rate, 5°C/min). In the range 100–250°C, the TG curve shows two consecutive weight losses in good agreement with the departures of the two types of water (theoretical 14.9% vs experimental 15.4%). The combustion of the organic part occurs above 500°C and leads to the destruction of the structure.

X-Ray Diffraction

The powder was finely ground in alcohol in a McCrown apparatus to homogenize the grain size, dried in air at 80°C, and vertically introduced in a McMurdie sample holder to limit the preferential orientation effects. The powder pattern was monitored at room temperature over the angular range 8.5–100° (2θ) with a step size of 0.02° using a D5000 Siemens diffractometer equipped with a secondary monochromator. The counting times were 30 s·step^{-1} to 41° (2θ) and 60 s.step^{-1} from 41 to 100°, in order to improve the counting statistic of the high-angle region.

The pattern was indexed with the DICVOL91 program (24); a body-centered orthorhombic solution was found for $(V^{IV}O)_2(H_2O)\{O_3P\text{-}(CH_2)_3\text{-}PO_3\}\cdot 2H_2O$ with the figures of merit $M/F(20) = 24.3/39.4$ (0.0085, 60). The systematic absences (hkl, $h + k + l = 2n + 1$) are in agreement with space group *Immm* and its subgroups *Imm*2 and *I*222. The structure was solved using *Immm* (No. 71). In the first step, the EXPO program (25) was used to adjust the pattern matching and to find a structure solution by a direct method. The refinement was then performed using Fullprof 97 (26). A pseudo-Voigt function was selected to adjust individual line profiles. In order to describe the angular dependence of the peak full-width at half-maximum, the usual quadratic function in $\tan\theta$ was used. Some interatomic distance constraints were applied at the beginning (P–O = 1.55 Å, P–C = 1.80 Å, C–C = 1.55 Å, V–O = 2.00 Å, V=O = 1.60 Å), and removed at the end of the refinement. The final Rietveld refinement using 375 F_{obs} involved the following parameters: one scale factor, 17 atomic coordinates, one overall isotropic thermal factor, one zero point and three cell parameters, three half-width parameters, two asymmetry factors, two parameters to define the θ-dependent pseudo-Voigt profile shape function, six coefficients to describe the functional dependence of the background, and one preferred orientation factor. The agreement factors defined in Refs. (27) and (28) were $R_P = 10.7\%$, $R_{wP} = 14.8\%$ (nonconventional Rietveld factors), $R_{Bragg} = 8.26\%$, $R_F = 9.29\%$. The corresponding final Rietveld plot is shown in Fig. 1.

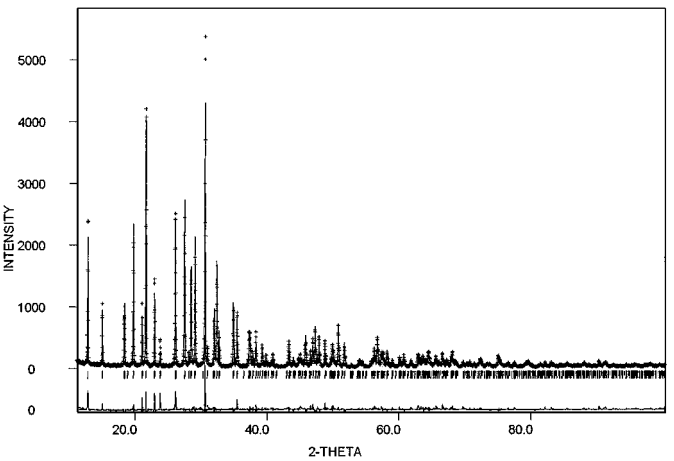

FIG. 1. Final Rietveld plot of the structure refinement of $(V^{IV}O)_2(H_2O)\{O_3P\text{-}(CH_2)_3\text{-}PO_3\}\cdot 2H_2O$ (the zone with the strongest peak was excluded).

The conditions of data measurements and the principal *d*-spacings are summarized in Tables 1 and 2, respectively. The atomic coordinates and the important bond lengths and angles are given in Tables 3 and 4, respectively.

TABLE 1
Conditions for Data Measurements and Crystal Data for $(V^{IV}O)_2(H_2O)\{O_3P\text{-}(CH_2)_3\text{-}PO_3\}\cdot 2H_2O$

Formula weight (g.mol^{-1})	388
Measured density (g.cm^{-3})	2.133(6)
Calculated density (g.cm^{-3})	2.191
Crystal system	Orthorhombic
Space group	*Immm* (No. 71)
Lattice parameters	$a = 16.8210(5)$ Å
	$b = 9.3790(3)$ Å
	$c = 7.4568(2)$ Å
	$V = 1176.4(1)$ Å^3
	$Z = 4$
Radiation (λCu (Å)): $K\alpha_1$, $K\alpha_2$	1.54059, 1.54439
Range of data collection (2θ, °)	8.5–100
h, k, l indices limits	$0 \le h \le 16$; $0 \le k \le 9$; $0 \le l \le 7$
Step size (°)	0.02
Time count per step	30 sec in the range $8.5 \le 2\theta \le 41°$
	60 sec in the range $41 \le 2\theta \le 100°$
Number of reflections	375
Number of profile points	4576
Number of refined parameters	37
Number of refined atoms	9
Preferred orientation	[100]
R_p(%)	10.7
R_{wp}(%)	14.8
R_{Bragg}(%)	8.26
R_F(%)	9.29

TABLE 2
Indexed Powder Pattern of $(V^{IV}O)_2(H_2O)\{O_3P\text{–}(CH_2)_3\text{–}PO_3\} \cdot 2H_2O$ (Limited to the Reflections with $I \geq 2\%$)

h	k	l	d_{obs} (Å)	Intensity (%)
2	0	0	8.4172	100
1	0	1	6.8292	4.2
3	0	1	4.4862	4.2
2	2	0	4.1019	7.8
1	2	1	3.8680	2.6
2	0	2	3.4136	4.8
3	2	1	3.2430	5.7
4	2	0	3.1329	3.3
5	0	1	3.0688	4.6
0	2	2	2.9208	11.8
4	0	2	2.7913	2.3
2	2	2	2.7595	3.5
5	2	1	2.5685	2.5
6	1	1	2.5291	2.5
4	4	2	1.7959	2.3

TABLE 4
Principal Bond Lengths (Å) and angles (°) in $(V^{IV}O)_2(H_2O)\{O_3P\text{–}(CH_2)_3PO_3\} \cdot 2H_2O$

$V_2^{IV}O_8(H_2O)$ dimers	Phosphonate units
V–V: 3.089(4)	P–O(3): 1.518(8) (2×)
V–O(2): 1.59(1)	P–O(1): 1.56(1)
V–O(3): 1.927(7) (2×)	P–C(2): 1.84(1)
V–O(1): 2.086(7) (2×)	O(1)–P–O(3): 107.2(8) (2×)
V–O(4)w: 2.365(9)	O(3)–P–O(3): 111.3(8)
O(1)–V–O(1): 80.1(6)	O(1)–P–C(2): 107(1)
O(1)–V–O(2): 96.8(6) (2×)	O(3)–P–C(2): 112.0(9) (2×)
O(1)–V–O(3): 156.0(6) (2×)	
O(1)–V–O(3): 90.1(4) (2×)	C(1)–C(2): 1.55(2) (2×)
O(1)–V–O(4)w: 70.3(5) (2×)	C(2)–C(1)–C(2): 101(1)
O(2)–V–O(3): 106.1(7) (2×)	
O(2)–V–O(4)w: 162.8(9)	
O(3)–V–O(3): 90.3(5)	
O(3)–V–O(4)w: 85.8(4) (2×)	

Magnetic Measurements

The magnetization (M) of the vanado-propylenediphosphonate sample was measured as a function of the temperature in the range 2–300 K with a Quantum Design Squid device, and then the resulting magnetic susceptibility $\chi = M/H$ was deduced (Fig. 4). Some supplementary measurements giving the magnetization versus the applied field H in the range 5–70 K were also performed to confirm the transition toward an antiferromagnetic state.

DISCUSSION

Structure Description

$(V^{IV}O)_2(H_2O)\{O_3P\text{–}(CH_2)_3\text{–}PO_3\} \cdot 2H_2O$ provides a new example of metallodiphosphonate exhibiting a pillared structure. The inorganic slabs stacking along [100] are joined by the propyl chains (Fig. 2). Each layer with a $V/P = 1$ stoichiometry is formed by the linkage of $[V_2^{IV}O_8(H_2O)]$ dimeric units and tetrahedral PO_3C phosphonate groups. Each dimer is built up from two face-shared $VO_5(H_2O)$ octahedra, inside which the short

TABLE 3
Atomic Coordinates and Esd's (×10⁴) for $(V^{IV}O)_2(H_2O)\{O_3P\text{–}(CH_2)_3\text{–}PO_3\} \cdot 2H_2O$

Atoms[a]	x	y	z
V (8*m*)	2439(2)	0	2929(4)
P (8*n*)	3296(3)	2669(6)	1/2
O(1) (8*n*)	2680(6)	1431(11)	1/2
O(2) (8*m*)	3307(6)	0	2072(13)
O(3) (16*o*)	3150(4)	3543(7)	6681(10)
O(4)w (4*f*)	1374(7)	0	1/2
Ow (8*n*)	831(4)	2650(11)	1/2
C(1) (4*g*)	1/2	2888(24)	1/2
C(2) (8*n*)	4289(7)	1838(15)	1/2

[a]The crystallographic sites are given in parentheses.

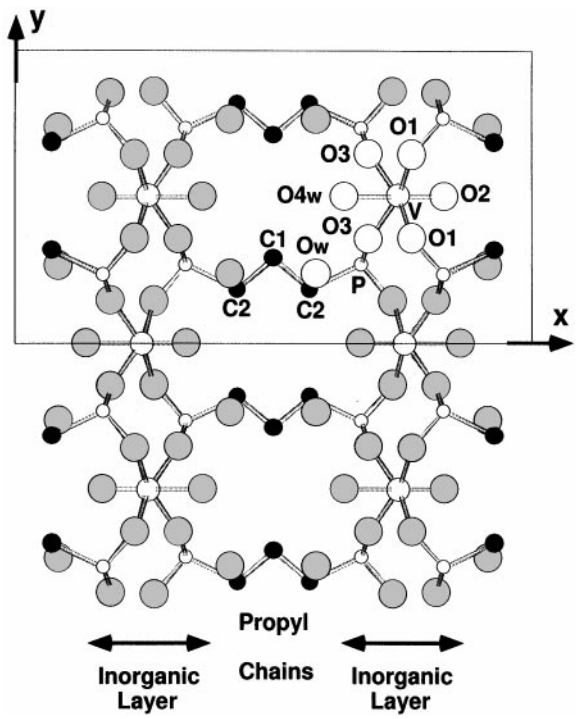

FIG. 2. Projection of the structure of $(V^{IV}O)_2(H_2O)\{O_3P\text{–}(CH_2)_3\text{–}PO_3\} \cdot 2H_2O$ along [001] showing its pillared character (ball stick model: large circles for O, black circles for C, small circles for P, and medium circles for V).

vanadyl bond V = O(2) is translocated to the water molecule (Table 3). Both the light blue color of the powder and the valence bond calculations (4.139 v.u.) according to the data of Brese and O'Keeffe (29) show unambiguously that vanadium is in the +IV oxidation state. The common face of the octahedral dimers is defined by two O(1) oxygen atoms and one water molecule O(4). An additional water molecule is intercalated between the layers. Three oxygen atoms of the phosphonate groups connect three bioctahedral dimers within a layer and the fourth apex occupied by a carbon atom points alternatingly up and down the layers in such a way that they ensure the three-dimensionality of the framework (Fig. 3) via the propyl chains.

The same type of inorganic layer was described in the bidimensional compound $VO(HPO_4)\cdot 0.5H_2O$ (23). The polyhedral network is the same but the C atoms of the phosphonate functions are substituted by terminal hydroxyl groups. Consequently, the framework is interrupted in the hydrogenphosphate and the structure becomes layered while in the title compound, two phosphonate groups of two adjacent layers are exactly face to face and ensure the connectivities between them (Fig. 2).

Magnetic Properties

The temperature dependence of the reciprocal magnetic susceptibility is given in Fig. 4. Its aspect is well known for this type of inorganic layer and was previously described for the phosphate $VO(HPO_4)\cdot 0.5H_2O$ (23) and the structurally

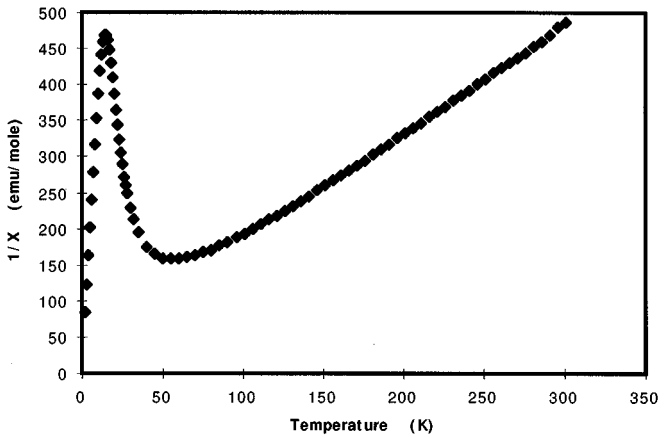

FIG. 4. Thermal evolution of the reciprocal magnetic susceptibility.

analogous selenite $VOSeO_3\cdot H_2O$ (30). After correction for diamagnetism, the linear part of the curve was fitted in the temperature range 150–300 K. It leads to a molar Curie constant $C = 0.795(1)$ and an effective magnetic moment of $1.78(1)\,\mu_B$, characteristic of V^{IV}. The small value of θ (-42 K) indicates weak antiferromagnetic interactions.

Owing to the structural characteristics, the low-temperature part of the curve was fitted using a model of dimers according to the Bleaney–Bowers equation $\chi_m = (2Ng^2\mu_B^2/kT)\,[3 + \exp(-2J/kT)]^{-1}$ or with an Ising model $\chi_m = (2Ng^2\mu_B^2/4kT)\exp(J/2kT)$. The first procedure (Fig. 5) is by far better than the second. It leads to the refined values $g = 1.984(2)$ and $J/k = -42.2(2)$ K, which give the model of

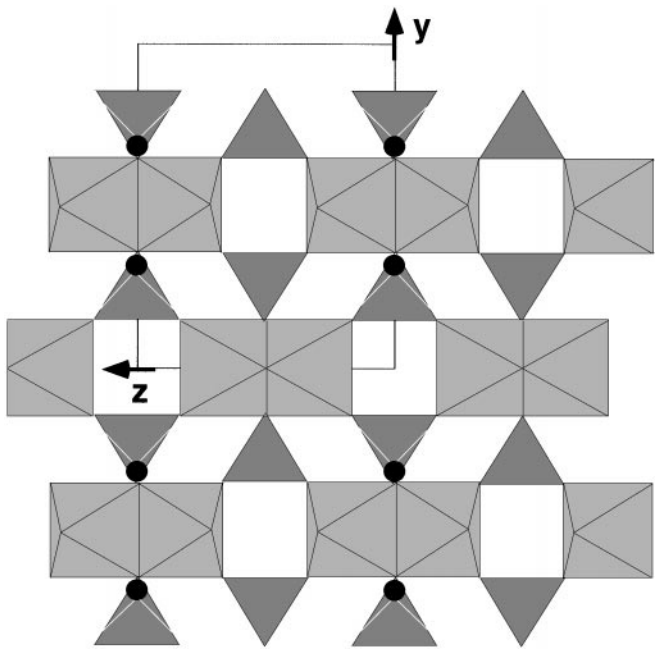

FIG. 3. Projection of one layer of $(V^{IV}O)_2(H_2O)\{O_3P{-}(CH_2)_3{-}PO_3\}\cdot 2H_2O$ along [100].

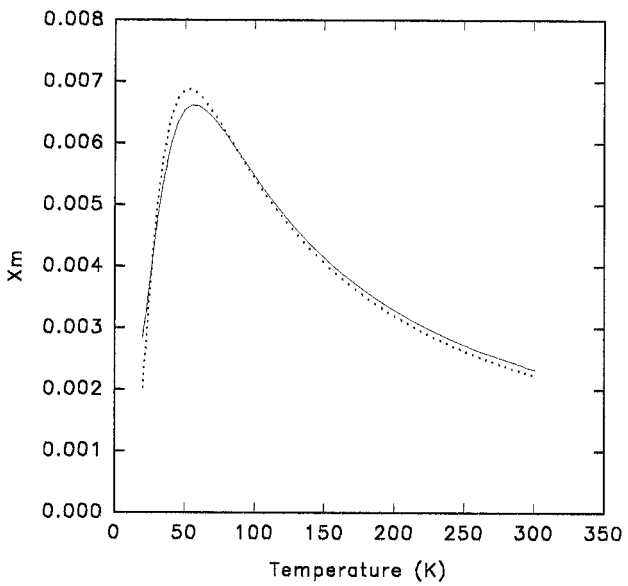

FIG. 5. Fit (dotted lines) against experimental data (full line) of the low-temperature part of the $\chi(T)$ curve using a model of dimers for the magnetic behavior.

dimers the magnetic behavior of the title compound. The two-dimensional parent phosphate $V^{IV}O(HPO_4)\cdot 0.5H_2O$ was fitted using the same model. The poorer fit of the title compound may find its origin in the fact that it exhibits a 3D structure via the alkyl chains, whereas $V^{IV}O(HPO_4)\cdot 0.5H_2O$ is 2D. Our 3D structure may induce a long-range weak magnetic interaction between the dimers which is not taken into account in the Bleaney–Bowers equation.

However, the modest quality of our fit cannot rule out the possibility of a spin ladder model for our compound, as already observed in the closely related $(VO)_2P_2O_7$ (31–34).

CONCLUSION

The three-dimensional pillared structure of $(V^{IV}O)_2(H_2O)\{O_3P\text{–}(CH_2)_3\text{–}PO_3\}\cdot 2H_2O$ show original features closely related to a hydrogenphosphate compound. It is shown that the terminal hydroxy group of the phosphate and the alkyl chain of the phosphonate units assume a similar role. This similarity between the two functions opens the way toward new pillared and/or microporous compounds with structures derived from metallo-hydrogenphosphates.

ACKNOWLEDGMENTS

The authors are indebted to Dr. M. Nogues (LMOV, Univ. of Versailles) for his help in magnetic measurements.

REFERENCES

1. A. K. Cheetham, G. Férey, and Th. Loiseau, *Angew. Chem.* **38,** 3248 (1999).
2. A. Clearfield, *Curr. Opin. Solid State Mater. Sci.* **1,** 268 (1996) and references therein.
3. C. Livage, C. Egger, M. Nogues, and G. Férey, *J. Mater. Chem.* **8,** 2743 (1998).
4. F. Serpaggi and G. Férey, *J. Mater. Chem.* **8,** 2737 (1998).
5. S. S. Y. Chui, S. M. F. Lo, J. P. H. Charmant, A. G. Orpen, and I. D. Williams, *Science* **283,** 1148 (1999).
6. (a) O. M. Yaghi, G. Li, and H. Li, *Nature* **378,** 703 (1995); (b) O. M. Yaghi, C. E. Davis, G. Li, and H. Li, *J. Am. Chem. Soc.* **119,** 2861 (1997).
7. F. Serpaggi and G. Férey, *J. Mater. Chem.* **8,** 2749 (1998).
8. M. Riou-Cavellec, C. Serre, J. Robino, M. Noguès, J. M. Grenèche, and G. Férey, *J. Solid State Chem.* **147,** 122 (1999).
9. W. T. A. Harrison, L. L. Dussack, and A. J. Jacobson, *Inorg. Chem.* **35,** 1461 (1996).
10. G. Huan, A. J. Jacobson, J. W. Johnson, and E. W. Corcoran, *Chem. Mater.* **2,** 91 (1990).
11. G. Huan, J. W. Johnson, A. J. Jacobson, and J. S. Merola, *J. Solid State Chem.* **89,** 220 (1990).
12. G. H. Bonavia, R. C. Haushalter, S. Lu, C. J. O'Connor, and J. Zubieta, *J. Solid State Chem.* **132,** 144 (1997).
13. M. I. Khan, Y. S. Lee, C. J. O'Connor, R. C. Haushalter, and J. Zubieta, *J. Am. Chem. Soc.* **116,** 4525 (1994).
14. M. I. Khan, Y. S. Lee, C. J. O'Connor, R. C. Haushalter, and J. Zubieta, *Chem. Mater.* **6,** 721 (1994).
15. M. I. Khan, Y. S. Lee, C. J. O'Connor, R. C. Haushalter, and J. Zubieta, *Inorg. Chem.* **33,** 3855 (1994).
16. V. Soghomonian, Q. Chen, R. C. Haushalter, and J. Zubieta, *Angew. Chem., Int. Ed. Engl.* **34** (2), 223 (1995).
17. G. Bonavia, R. C. Haushalter, C. J. O'Connor, and J. Zubieta, *Inorg. Chem.* **35,** 5603 (1996).
18. V. Soghomonian, R. C. Haushalter, and J. Zubieta, *Chem. Mater.* **7,** 1648 (1995).
19. D. Riou, O. Roubeau, and G. Férey, *Microporous Mesoporous Mater.* **23,** 23 (1998).
20. C. Ninclaus, C. Serre, D. Riou, and G. Férey, *C. R. Acad. Sci. Paris* **II**(1), 551 (1998).
21. D. Riou, C. Serre, and G. Férey, *J. Solid State Chem.* **141,** 89 (1998).
22. D. Riou and G. Férey, *J. Mater. Chem.* **8,** 2733 (1998).
23. M. E. Leonowicz, J. W. Johnson, J. F. Brody, H. F. Shannon, and J. M. Newsam, *J. Solid State Chem.* **56,** 370 (1985).
24. A. Boultif and D. Louer, *J. Appl. Crystallogr.* **24,** 987 (1991).
25. (a) A. Altomare, M. C. Burla, G. Cascarano, A. Guagliardi, A. G. G. Moliterni, and G. Polidori, *J. Appl. Crystallogr.* **28,** 842 (1995); (b) A. Altomare, G. Cascarano, C. Giacovazzo, A. Guagliardi, M. C. Burla, G. Polidori, and M. Camalli, *J. Appl. Crystallogr.* **27,** 435 (1994).
26. J. Rodriguez-Carjaval, "Collected Abstracts of Powder Diffraction Meeting," p. 127. Toulouse, France, 1990.
27. R. A. Young and D. B. Wiles, *J. Appl. Crystallogr.* **15,** 430 (1982).
28. R. A. Young, *Proc. Egyptian 3rd Int. School Crystallogr.* (*Cairo*) 60 (1990).
29. N. E. Brese and M. O'Keeffe, *Acta Crystallogr. B* **47,** 192 (1991).
30. G. Huan, J. W. Johnson, A. J. Jacobson, D. P. Goshorn, and J. S. Merola, *Chem. Mater.* **3,** 539 (1991).
31. D. C. Johnston, J. W. Johnson, D. P. Goshorn, and A. J. Jacobson, *Phys. Rev. B* **35,** 219 (1987).
32. R. S. Eccleston, T. Barnes, J. Brody, and J. W. Johnson, *Phys. Rev. Lett.* **73,** 2626 (1994).
33. T. Barnes and J. Rieira, *Phys. Rev. B* **50,** 6817 (1994).
34. J. Kikuchi, T. Yamauchi, and Y. Ueda, *J. Phys. Soc. Jpn.* **66,** 1622 (1997).